参赛学生姓名：陈禹翔

中学：北京一零一中（北京市第一〇一中学）

省份：北京

国家/地区：中国

指导老师姓名：张雨桐

指导老师单位：北京一零一中

论文题目:Campus Fire Outdoor Evacuation Plan Design: Taking Beijing 101 High School as an Example

2026 S.T.Yau High School Science Award
仅用于2026丘成桐中学科学奖论文公示

Campus Fire Outdoor Evacuation Plan Design: Taking Beijing 101 High School as an Example

Yuxiang Chen (Lambert)
Beijing 101 High School International Department
High School Student
Beijing, China
c19801354136@outlook.com

***Abstract*—This study proposes a GIS-based framework for safer outdoor campus fire evacuation by coupling hazardous-gas generation, wind-driven advection–diffusion, and route optimization. Taking Beijing 101 High School as the case area, the campus is modeled as a road-network graph. CO, HCN, and HCl released are estimated from combustible material mass, converted into time-dependent source terms, and propagated on a finite-difference grid. Evacuation paths are then evaluated by FED-based exposure, route length, bottleneck road width, and assembly-point capacity. The case simulation shows that the safest route can differ from the geometric shortest route when plume direction, departure time, road width, and destination capacity are considered together.**

***Index Terms*—Campus fire evacuation; Hazardous gas diffusion; Wind-driven advection-diffusion; FED exposure; GIS road network; Route optimization**

I. Introduction

Existing school evacuation planning under fire circumstances commonly separates smoke or toxic-gas analysis from people evacuating route selection. Atmospheric-dispersion models can describe the transport of released substances under diffusion and wind advection [1], while graph-based methods can identify the shortest or the most low-cost paths [2], However, a campus plan must use these components together: the gas field changes with time, people start evacuating at different locations, and assembly points have finite capacity. These interactions motivate the following research question: *how can a campus road network be converted into evacuation recommendations that account simultaneously for time-dependent toxic exposure, travel distance, road bottlenecks, and destination capacity?*

This study develops a reproducible scenario-simulation framework to address that question. First, a simplified combustion model estimates the release of CO, HCN, and HCl from selected combustible-material list. Second, a wind-driven two-dimensional advection-diffusion model calculates the resulting source terms on a finite-difference grid. Third, the computed concentration field is sampled along candidate paths in a GIS road network and combined with FED-based exposure, path length, bottleneck width, and assembly-point constraints. The framework is demonstrated with a Beijing 101 High School case study with a Yingcai College fire scenario.

II. Notations and Parameters

Several critical symbols and parameters are defined in Table I.

TABLE I: Symbols and parameters used throughout the paper

Symbol	Description	Unit / type
Geographical Information and Road Network Graph		
$\mathcal{G}$; $\mathcal{V}, \mathcal{E}$	Road graph; node/edge sets	Graph; sets
v_k	Node	Node
e_m	Edge	Edge
id_k	Node ID	ID
x, y	Node ground coordinates	m
$dist_m$	Edge length	m
$label_k$	Node labels	Text
id_m	Edge ID	ID
P_k	Node population	Integer
W_m	Walkable width	m
General Field, Grid, and Operators		
$t, \tau, \Delta t$	Simulation/elapsed time, time step	s
t_{evac}	Departure times	s
i, j; i_s, j_s	Grid, source cells	Integers
Model 1: Gas Generation Model		
g	Gas species $\in \{CO, HCN, HCl\}$	Type
q_g	Mass-specific gas generation rate	$\mathrm{kg\,s^{-1}\,kg^{-1}}$
M_g	Fuel mass	kg
$m_g(t)$	Generated gas mass	kg
Model 2: Gas Advection-Diffusion Model		
A_s	Effective source area	$\mathrm{m^2}$
S_g	Gas source term	$\mathrm{kg\,m^{-2}\,s^{-1}}$
C_g	Continuous concentrations field	$\mathrm{kg\,m^{-2}}$
$\widehat{C}_g$	Discrete grid concentrations	$\mathrm{kg\,m^{-2}}$
$D_{\text{eff},g}$	Effective diffusivity	$\mathrm{m^2\,s^{-1}}$; $\mathrm{s^{-1}}$
λ_g	Attenuation coefficient	$\mathrm{s^{-1}}$
$\vec{w} =< u, v >$	Wind vector	$\mathrm{m\,s^{-1}}$
Model 3: Route Optimization Model		
$\mathcal{P}_k$	Feasible candidate-path set	Set
$p_{h,k}, p_k^*$	Candidate / Optimal path	Path
s	Walking speed	$\mathrm{m\,s^{-1}}$; m, s
$L(p_{h,k}), T(p_{h,k})$	Route length/time	m; s
$x_{p_{h,k}}(\tau), y_{p_{h,k}}(\tau)$	Evacuee position along a path	m
$\widehat{H}_g$	Literature reference toxic dose	ppm min
H_g	Converted 2D reference toxic dose	$\mathrm{kg\,s\,m^{-2}}$
FED(t)	Total time dose	Dimensionless
$E(p_{h,k})$	Route exposure	Dimensionless
$W_{\min}(p_{h,k})$	Narrowest edge width on a path	m
L_0	Length reference	m
E_0	Exposure reference	Unitless
W_0	Width reference	m
α, β, γ	Length, exposure, width weights	Dimensionless
Cost$(p_{h,k})$	Normalized comprehensive route cost	Dimensionless

2025 Siyuan Cup · Yali High School Science Award
仅用于2025年第十一届雅礼杯科学奖公示

III. Overall Model Framework

The overall framework of this study is a connected models chain: begin at fire chemistry, going to hazardous gas advection-diffusion behavior, and finally evacuation paths optimization. The complete model chain is summarized in Fig. 1.

First, **model 1** simplifies the combustion process of building materials into a hazardous gas generation function, which estimates the mass $m_g(t)$ of gas species g generated by time t.

Second, **model 2** converts the mass function into the source term $S_g(t)$ that is used in the diffusion model. Then, $S_g(t)$ is inserted into a two-dimensional advection-diffusion equation with wind influence based on Fick's law. This model describes the outdoor spread of hazardous gas on campus using the continuous concentration field $C_g(x, y, t)$, which is discretized into grid-based concentrations $\widehat{C}_g(i, j, t)$ through a finite-difference method, and the size of each grid are define as Δx and Δy. The wind field in the diffusion equation is represented as a two-dimensional vector field $\vec{w}(x, y) = \langle u(x, y), v(x, y) \rangle$, and in the discrete grid it is denoted as $\vec{w}_{i,j} = \langle u_{i,j}, v_{i,j} \rangle$. The main output of Model 2 is the time-dependent concentration distribution.

Thirdly, **model 3** combines the concentration field produced by Model 2 with the real campus road network graph. For each people cluster k, the model compares candidate paths $p_{h,k}$ within the feasible path set $\mathcal{P}_k$. The cost of a path depends on its total distance $L(p_{h,k})$, total exposure value $E(p_{h,k})$ in the FED method, and the narrowest road width $W_{\min}(p_{h,k})$ along the path by the main function $\textbf{Cost}(p_{h,k}) = \alpha \frac{L(p_{h,k})}{L_0} + \beta \frac{E(p_{h,k})}{E_0} + \gamma \frac{W_0}{W_{\min}(p_{h,k})}$. A path with a smaller bottleneck width receives a larger width penalty. Therefore, the evacuation problem is transformed into a comprehensive cost minimization problem.

This chain connects the chemical, numerical, and algorithmic components. The output p_k^* is the minimum-cost feasible path selected from the candidate paths for cluster k. The study therefore combines combustion chemistry, numerical calculus, GIS, and graph-based optimization.

$$\underbrace{t \to m_g(t)}_{\text{Model 1}} \to \underbrace{S_g(t) \to \widehat{C}_g(i,j,t)}_{\text{Model 2}} \to \underbrace{E(p_{h,k}) + L(p_{h,k}) + W_{\min}(p_{h,k}) \to \text{Cost}(p_{h,k}) \to p_k^*}_{\text{Model 3}} \tag{1}$$

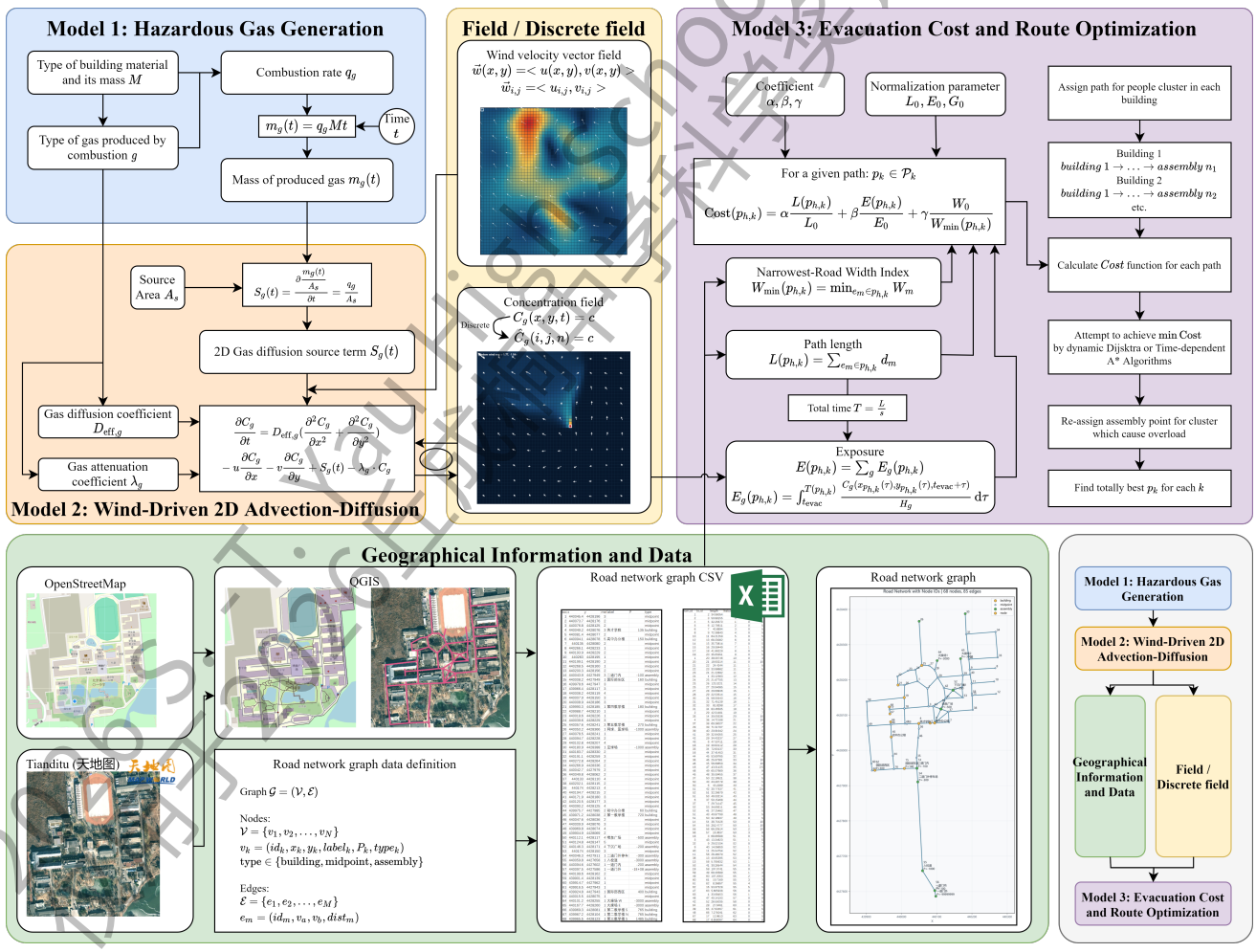


Fig. 1: Model Framework

2026 Sci-Tech Undergraduate Research Award 校内科技论文公开

IV. Data Sources and Preprocessing

A. Geographical Map

The geographical map of the school can be obtained from geographical data supplier, such as *OpenStreetMap*. Then, Geographical features are abstracted into a graph structure, denoted as $\mathcal{G}$ and defined as:

$$\mathcal{G} = (\mathcal{V}, \mathcal{E}) \tag{2}$$

The graph abstraction used in the case study is shown in Fig. 2. Its mathematical graph structure and campus geographic map are shown in Fig. 2a and Fig. 2b, respectively.

1) Nodes: Nodes v_k are defined to represent key locations on campus. Each one node is defined as:

$$v_k = (id_k, x_k, y_k, label_k, P_k, type_k) \tag{3}$$

Which:

- id_k: Unique identifier for node v_k;
- (x_k, y_k): Spatial coordinates of node v_k;
- $label_k$: Descriptive label for node v_k (e.g., "Building A Exit", "Assembly Point 1");
- P_k: Population assigned to node v_k (if applicable, positive for buildings nodes and negative for assembly points);
- $type_k$: Categorical variable indicating the type of node (e.g., "building", "midpoint", "assembly").

According to the geographical components, the list of node types include building nodes (`"building"`), road midpoints (`"midpoint"`), and assembly points (`"assembly"`).

2) Edges: Edges e_m represent the straight walkable paths between nodes, which are obtain and simplified from the road segments from the geographical data. Each edge is defined as:

$$e_m = (id_m, v_a, v_b, dist_m, W_m) \tag{4}$$

Which:

- id_m: Unique identifier for edge e_m;
- v_a, v_b: The two nodes that edge e_m connects, which can be passed by two direction;
- $dist_m$: The distance of edge e_m, used directly in path-length calculations;
- W_m: The effective walkable width of edge e_m, obtained from the road-width attribute in the geographical data or assigned from a default width when this attribute is missing.

The width attribute is used directly in Model 3. A smaller value of W_m means that the road segment is narrower and more likely to become a bottleneck during evacuation. Therefore, the path-level bottleneck is measured by the narrowest edge width instead of by a separate carrying-capacity variable.

$$W_{\min}(p_{h,k}) = \min_{e_m \in p_{h,k}} W_m \tag{5}$$

B. Wind Field

The wind field $\vec{w}(x, y) = \langle u(x, y), v(x, y) \rangle$ is obtained from local meteorological data, which provides information about the wind speed and direction on campus. The continuous wind field is discretized into a grid-based representation $\vec{w}_{i,j} = \langle u_{i,j}, v_{i,j} \rangle$ that corresponds to the grid used in the diffusion model.

To simplify the model, the wind field is assumed to be uniform across the campus. It is represented by a constant vector $\vec{w} = \langle u, v \rangle$, where u and v are the wind components along the local x- and y-axes. Thus, $\vec{w}_{i,j} = \vec{w}$ for every grid cell.

V. Model 1: Hazardous Gas Generation Model

This model estimates the time-dependent release of selected gases from a simplified combustible-material list.

A. Building Material and Its Combustion Product

Combustion products depend on fuel composition and ventilation. Carbon monoxide (CO) is a colorless product of incomplete combustion that can spread over a broad downwind region and remain a persistent exposure hazard [3]. Hydrogen cyanide (HCN) is mainly generated from nitrogen-containing materials. Although transported similarly to CO, its lower toxic threshold can produce significant FED exposure even at moderate concentrations [3, 4]. Hydrogen chloride (HCl) is primarily produced from PVC and other chlorine-containing materials. As an irritant gas, its impact is strongest near the fire source and generally decreases more rapidly through outdoor dilution [3].

These three gases are usually generated during combustion with considerable toxic. [4, 5, 6]. Thus, the are selected in the toxic gas list.

B. Generation Rate q_g of gas g

After identifying the main hazardous gases, the next step is to estimate the generation rate q_g of each gas g. In this scenario model, q_g is treated as a constant mass-specific generation rate with unit $\mathrm{kg\,s^{-1}\,kg^{-1}}$, and M_g denotes the corresponding combustible-material mass.

Because the material loss is small relative to its assumed inventory during the short evacuation interval, M_g is treated as constant. The generation rate is therefore:

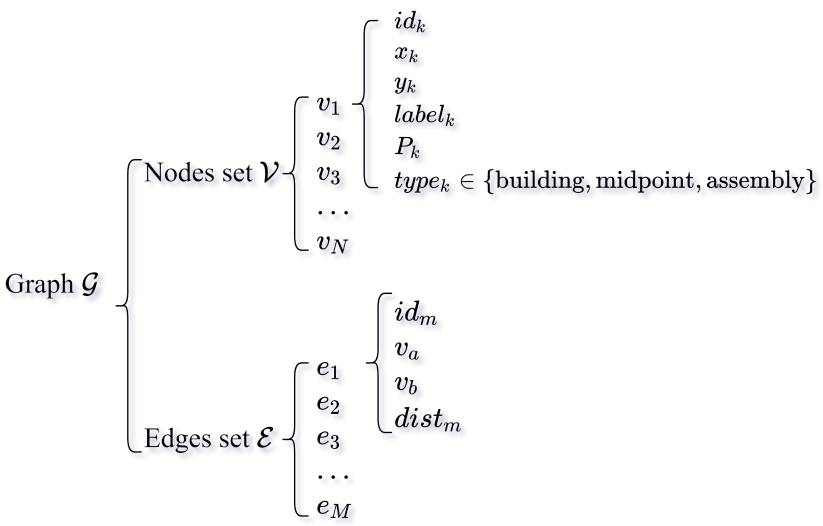
$$\frac{\mathrm{d}m_g(t)}{\mathrm{d}t} = q_g M_g \tag{6}$$

The total mass generated by time t is:

$$m_g(t) = \int_0^t q_g M_g \,\mathrm{d}t = q_g M_g t \tag{7}$$

Thus, the model uses a linear source-mass approximation over the simulated interval. The values of q_g for chosen gas are shown below:

2026 S. T. Yau High School Science Award
第十八届2026丘成桐中学科学奖



(a) Geographical Map Structure Represent in Math



(b) Geographical Map of Beijing 101

Fig. 2: Campus Geographic Data and Graph Abstraction

VI. Model 2: Wind-Driven 2D Advection-Diffusion Model

This model is aimed at describing the outdoor diffusion of hazardous gas on campus under the influence of the wind field $\vec{w}(x, y) = \langle u, v \rangle$. Its output is the concentration distribution $C_g(x, y, t)$ of gas g at location (x, y) and time t. The finite-difference field $\widehat{C}_g(i, j, t)$ denotes the cell-average concentration in grid cell (i, j), whose center is (x_i, y_j); t is the simulation time. The wind field is discretized as $\vec{w}_{i,j} = \langle u_{i,j}, v_{i,j} \rangle$.

A. Source Term Construction

In the two-dimensional diffusion field, the burning building is simplified as the source of hazardous gas. The effective source area A_s is defined according to the area of each grid cell:

$$A_s = \begin{cases} \text{building footprint area}, & \text{building-footprint source}, \\ \Delta x \Delta y, & \text{single-grid source} \end{cases} \tag{8}$$

Then, the area-averaged source strength is defined as:

$$S_g(t) = \frac{1}{A_s} \frac{\mathrm{d}m_g(t)}{\mathrm{d}t} = \frac{q_g M_g}{A_s} \tag{9}$$

The unit of $S_g(t)$ is kg/(m^{2}s), which is consistent with the two-dimensional concentration unit kg/m^2. The continuous source is $S_g(x, y, t) = S_g(t)$ inside the selected source area and zero elsewhere; (i_s, j_s) is the grid cell containing that area, so the discrete source is applied only there:

$$S_g(i, j, t) = \begin{cases} \dfrac{q_g M_g}{A_s}, & (i, j) = (i_s, j_s), \\ 0, & (i, j) \neq (i_s, j_s) \end{cases} \tag{10}$$

This treatment means that the gas is only generated at the building source location instead of being added uniformly to the whole campus area.

B. Fick's Law and its Expression in Advection-Diffusion Equation

Fick's law is the foundation of the diffusion model, which states that the flux of a substance is proportional to the negative gradient of its concentration. In the context of hazardous gas diffusion, Fick's law can be expressed as:

$$\vec{J}_g = -D_{\text{eff},g} \nabla C_g \tag{11}$$

- $\vec{J}_g$: Diffusive flux of gas species g in the two-dimensional field (kg·m^{-1}·s^{-1}).
- $D_{\text{eff},g}$: Effective diffusion coefficient of gas species g in the medium (m^2·s^{-1}).
- C_g: Two-dimensional concentration of gas species g (kg·m^{-2}).
- ∇C_g: Concentration gradient of gas species g in the two-dimensional field (kg·m^{-3}).
- $-$: Indicates that diffusion occurs from regions of higher concentration to regions of lower concentration.

Because the process happens in a two-dimensional outdoor environment and the effect of wind is significant, the diffusion

2026 S.-T. Yau High School Science Award 以用于2026丘成桐科学奖论文评选

process is modeled as a wind-driven advection-diffusion process. Under the assumption that the wind field is steady during the short-term evacuation process, the governing equation is

$$\frac{\partial C_g}{\partial t} = \underbrace{D_{\text{eff},g}\left(\frac{\partial^2 C_g}{\partial x^2} + \frac{\partial^2 C_g}{\partial y^2}\right)}_{\text{Diffusion Term}} \underbrace{-(u\frac{\partial C_g}{\partial x} + v\frac{\partial C_g}{\partial y})}_{\text{Advection Term}} + \underbrace{S_g(x,y,t)}_{\text{Source Term}} - \underbrace{\lambda_g C_g}_{\text{Decay Term}} \tag{12}$$

- $\frac{\partial C_g}{\partial t}$: The rate of change of concentration of gas g with respect to time t.
- $D_{\text{eff},g}(\frac{\partial^2 C_g}{\partial x^2} + \frac{\partial^2 C_g}{\partial y^2})$: The diffusion term, which represents the spreading of gas g due to concentration gradients. $D_{\text{eff},g}$ is the effective diffusion coefficient for gas g.
- $-u\frac{\partial C_g}{\partial x} - v\frac{\partial C_g}{\partial y}$: The advection term, which represents the transport of gas g due to the wind field. u and v are the wind velocity components in the x and y directions, respectively.
- $S_g(x,y,t)$: The source term, which represents the generation of gas g from the fire source location, as calculated in Model 1.
- $-\lambda_g \cdot C_g$: The decay term, which represents the natural decay or removal of gas g over time, where λ_g is the decay coefficient for gas g.

From the original partial differential Equation 12, the integral form can be derived as follows:

$$C_g(x,y,t) = C_g(x,y) + \int_0^t \Big[D_{\text{eff,g}}\frac{\partial^2 C_g}{\partial x^2} + D_{\text{eff,g}}\frac{\partial^2 C_g}{\partial y^2} - (u\frac{\partial C_g}{\partial x} + v\frac{\partial C_g}{\partial y}) + S_g(x,y,\tau) - \lambda_g C_g \Big] \mathrm{d}\tau \tag{13}$$

For numerical calculation, the diffusion terms are approximated by central differences. The advection terms are approximated by a first-order upwind scheme, because the direction of wind determines which neighboring cell contributes to the concentration transported into the current cell. The update equation is

$$\begin{aligned}\widehat{C}_g(i,j,t+\Delta t) = {} & \widehat{C}_g(i,j,t) \\ & + \Delta t\Big[D_{\text{eff},g}\Big(\frac{\widehat{C}_g(i+1,j,t) - 2\widehat{C}_g(i,j,t) + \widehat{C}_g(i-1,j,t)}{\Delta x^2} \\ & + \frac{\widehat{C}_g(i,j+1,t) - 2\widehat{C}_g(i,j,t) + \widehat{C}_g(i,j-1,t)}{\Delta y^2}\Big) \\ & - (u\delta_x^{\text{up}}\widehat{C}_g(i,j,t) + v\delta_y^{\text{up}}\widehat{C}_g(i,j,t)) \\ & + S_g(i,j,t) - \lambda_g\widehat{C}_g(i,j,t)\Big]\end{aligned} \tag{14}$$

The variables and terms in Equation 14 are explained as follows:

- $\widehat{C}_g(i,j,t+\Delta t)$: Concentration of gas g in grid cell (i,j) at the next time $t+\Delta t$, which is the value to be updated.
- $\widehat{C}_g(i,j,t)$: Concentration of gas g in grid cell (i,j) at the current time t.
- Δt: Time-step size used in the explicit finite-difference update.
- $D_{\text{eff},g}$: Effective diffusion coefficient of gas g, including molecular diffusion and outdoor turbulent mixing.
- Δx and Δy: Grid spacing in the x and y directions.
- The two long fractions: Central-difference approximations of the second derivatives in the diffusion term.
- u and v: Wind velocity components in $\vec{w} = \langle u, v\rangle$, representing wind-driven transport in the x and y directions.
- $\delta_x^{\text{up}}\widehat{C}_g(i,j,t)$ and $\delta_y^{\text{up}}\widehat{C}_g(i,j,t)$: Upwind derivatives, defined by $\delta_x^{\text{up}}\widehat{C}_g = (\widehat{C}_g(i,j,t) - \widehat{C}_g(i-1,j,t))/\Delta x$ for $u \geq 0$, otherwise $(\widehat{C}_g(i+1,j,t) - \widehat{C}_g(i,j,t))/\Delta x$; δ_y^{up} is defined analogously using v and Δy.
- $S_g(i,j,t)$: Discrete source term of gas g in grid cell (i,j) at time t, equal to $q_g M_g/A_s$ in the source cell and zero elsewhere.
- $\lambda_g\widehat{C}_g(i,j,t)$: Decay term of gas g, representing natural decay or removal of concentration during one time step.

C. Initial and Boundary Conditions

At the beginning of the diffusion process, the outdoor concentration of each hazardous gas is assumed to be zero over the whole computational domain. The grid-cell center is $(x_i, y_j) = (x_0 + i\Delta x, y_0 + j\Delta y)$.

$$C_g(x,y,0) = 0, \qquad \widehat{C}_g(i,j,t=0) = 0 \tag{15}$$

The computational domain is the rectangular area covering the campus and its nearby outdoor region. For the boundary of this domain, an open boundary condition is adopted. This means that gas can leave the simulation area freely, and no additional hazardous gas enters from outside the domain. In the finite-difference grid, this open boundary is approximated by a zero-gradient boundary:

$$\frac{\partial C_g}{\partial \mathbf{n}} = 0, \tag{16}$$

where $\mathbf{n}$ is the outward normal direction of the boundary. For a rectangular grid with N_x cells in the x direction and N_y cells in the y direction, this can be implemented as

$$\begin{aligned}&\widehat{C}_g(0,j,t) = \widehat{C}_g(1,j,t), \quad \widehat{C}_g(N_x+1,j,t) = \widehat{C}_g(N_x,j,t), \\ &\widehat{C}_g(i,0,t) = \widehat{C}_g(i,1,t), \quad \widehat{C}_g(i,N_y+1,t) = \widehat{C}_g(i,N_y,t)\end{aligned} \tag{17}$$

After each update, if a very small negative concentration is produced by numerical error, it is corrected by

$$\widehat{C}_g(i,j,t+\Delta t) = \max(\widehat{C}_g(i,j,t+\Delta t), 0) \tag{18}$$

2026 - Yau Hing School Science Award 仅用于2026年香港中学科学奖论文公开

D. Numerical Stability

Because Equation 14 is an explicit time-marching scheme, the time step Δt must be chosen carefully. A large time step may cause numerical oscillation or negative concentration. A simple and conservative time-step limit is

$$\Delta t \le \eta \min\left(\frac{\min(\Delta x^2, \Delta y^2)}{4D_{\text{eff},g}}, \frac{\Delta x}{|u|_{\max}}, \frac{\Delta y}{|v|_{\max}}\right), \quad 0 < \eta < 1 \tag{19}$$

Here $|u|_{\max}$ and $|v|_{\max}$ are the maximum absolute wind components over the computational domain and simulation interval; for the uniform-wind case, they equal $|u|$ and $|v|$.

The min function means that all stability restrictions are considered at the same time, and the smallest allowable value is selected. The first term, $\frac{\min(\Delta x^2, \Delta y^2)}{4D_{\text{eff},g}}$, is the diffusion restriction. It prevents gas diffusion from spreading too far within one time step. Smaller grid spacing or a larger effective diffusion coefficient requires a smaller Δt.

The second term, $\frac{\Delta x}{|u|_{\max}}$, is the advection restriction in the x direction. It means that the wind-driven transport in one time step should not exceed one grid spacing Δx. Similarly, the third term, $\frac{\Delta y}{|v|_{\max}}$, is the advection restriction in the y direction.

The parameter η is a safety factor between 0 and 1. It makes the selected time step slightly smaller than the theoretical upper limit, which improves numerical robustness when the wind field, source term, or grid resolution changes. If $|u|_{\max} = 0$ or $|v|_{\max} = 0$, the corresponding advection restriction can be ignored.

VII. Model 3: Evacuation Cost and Route Optimization Model

Model 3 connects the gas concentration field from Model 2 with the campus road network graph. The purpose of this model is to compare different evacuation paths for each people cluster and select the path with the lowest comprehensive evacuation cost. According to the overall framework, the cost of a path is determined by three parts: route length, toxic gas exposure, and the narrowest-road width penalty.

A. Candidate Path Set

For a people cluster k, the starting point is its building node, h indexes candidate routes, and the destination is a feasible assembly point. The candidate-path set is:

$$\mathcal{P}_k = \{p_{1,k}, p_{2,k}, \ldots, p_{h,k}, \ldots\} \tag{20}$$

Each candidate path $p_{h,k} \in \mathcal{P}_k$ is a connected sequence of road-network edges from the starting building node to an assembly point. A path is considered feasible only if all edges on the path are walkable and the destination assembly point has enough capacity for the assigned population. Therefore, assembly point capacity is treated as a feasibility condition rather than an additional term in the objective function, so the final cost structure remains consistent with the model framework.

TABLE II: Baseline reference toxic dose $\widehat{H}_g$ for FED-based exposure

Gas	$\widehat{H}_g$ in ppm·min	Basis
CO	2.83×10^4	Equivalent 30 min dose obtained from the FDS/Purser CO FED formula.
HCN	2.73×10^3	Equivalent 30 min dose obtained from the FDS/Purser cyanide FED formula without NOx correction.
HCl	1.14×10^5	Irritant fractional lethal dose FLD_{HCl} used in the FDS FED/FIC formulation.

Figure 3 illustrates five representative candidate routes from Yingcai College to distinct assembly points under the standard case settings. One minimum-cost candidate per displayed destination is shown to illustrate the branching structure of $\mathcal{P}_k$, before joint capacity assignment.

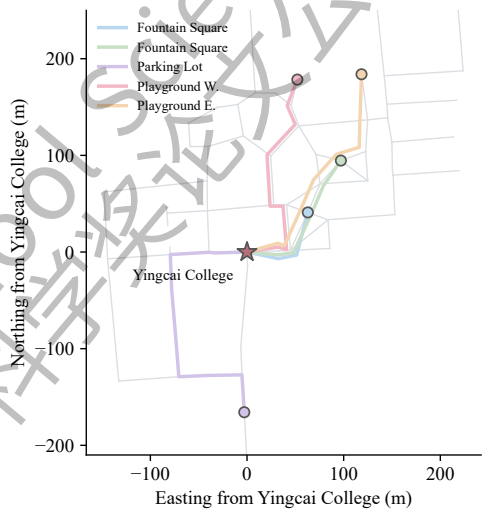


Fig. 3: Representative candidate routes from Yingcai College. The star marks the origin and colored circles mark assembly points. Coordinates are relative to the origin. Small lateral offsets separate overlapping routes for display only.

B. Path Length and Travel Time

The route length is calculated by summing the distances of all road edges contained in the path:

$$L(p_{h,k}) = \sum_{e_m \in p_{h,k}} dist_m \tag{21}$$

Assuming that the average evacuation speed of the crowd is s, the total travel time of the candidate path is estimated by:

$$T(p_{h,k}) = \frac{L(p_{h,k})}{s} \tag{22}$$

This time value is used to determine how long the people cluster is exposed to the hazardous gas field while moving along the path.

2026 S.T. Yau High School Science Award
仅用于2026丘成桐中学科学奖论文公示

C. FED-Based Exposure

The exposure value is calculated from the concentration field generated by Model 2. The Fractional Effective Dose (FED) method estimates toxic hazard by accumulating small exposure fractions over time. [3, 7]

Because Model 2 uses a two-dimensional mass concentration $C_g(x, y, t)$, while the FED literature usually gives reference doses in ppm·min, a unit conversion is needed before the exposure ratio is calculated. Let $\widehat{H}_g$ be the literature reference dose in ppm·min; P_{atm}, μ_g, R_{gas}, and T_{air} denote atmospheric pressure, gas molar mass, the ideal-gas constant, and air temperature, respectively.

$$\rho_{g,\text{ppm}} = 10^{-6} \frac{P_{\text{atm}} \mu_g}{R_{\text{gas}} T_{\text{air}}} \quad \text{kg/m}^3 \tag{23}$$

In this study, the harmful gas is assumed to be mixed within a breathing-zone height of $h_{\text{mix}} = 2\,\text{m}$. Therefore, the two-dimensional reference toxic dose inserted into the model is shown below, where the 60 factor converts minutes to seconds:

$$H_g = \widehat{H}_g \cdot 60 \cdot h_{\text{mix}} \cdot 10^{-6} \frac{P_{\text{atm}} \mu_g}{R_{\text{gas}} T_{\text{air}}}, \tag{24}$$

After this conversion, H_g has unit kg·s/m^2, which is consistent with $C_g \Delta t$. The general FED principle can be written in a simplified additive form:

$$\text{FED}(t) = \sum_g \frac{1}{H_g} \int_0^t C_g(\tau)\, \mathrm{d}\tau, \tag{25}$$

Where $C_g(\tau)$ is the concentration encountered by the evacuee and H_g is the reference toxic dose for gas g. The gas contributions are combined additively to obtain a comparable path-risk score:

$$E_g(p_{h,k}) = \frac{1}{H_g} \int_0^{T(p_{h,k})} \widehat{C}_g(x_{p_{h,k}}(\tau), y_{p_{h,k}}(\tau), \tau)\, \mathrm{d}\tau \tag{26}$$

Totally, the exposure score of a candidate path is the sum of contributions from all three hazardous gases:

$$E(p_{h,k}) = \sum_{g \in \{\text{CO,HCN,HCl}\}} E_g(p_{h,k}) \tag{27}$$

The baseline literature values $\widehat{H}_g$ in ppm·min are listed in Table II; they are converted to the two-dimensional H_g by the mixing-height formula before exposure calculation.

Thus, Table II gives the toxicological baseline $\widehat{H}_g$, while the numerical value inserted into the model is the converted H_g that follows the concentration unit used by Model 2.

In discrete calculation, each straight section of a road polyline is divided into segments by the boundaries of grids. Let r represent each segment within edge e_m. The implemented exposure score is:

$$E(p_{h,k}) \approx \sum_g \left(\frac{1}{H_g} \sum_{e_m \in p_{h,k}} \sum_{r \in e_m} \widehat{C}_g(i_{m,r}, j_{m,r}, t_{m,r}) \cdot \frac{\ell_{m,r}}{s} \right) \tag{28}$$

Here, $t_{m,r}$, the enter time of the segment r of edge e_m. $\widehat{C}_g$ denotes the corresponding interpolated concentration while the people cluster k is in the grid cell $(i_{m,r}, j_{m,r})$. $\ell_{m,r}$ is the length of the segment r of edge e_m with in the grid cell $(i_{m,r}, j_{m,r})$, and s is the average walking speed of the evacuee. Thus, summarized, this equation means that the exposure is accumulated over each segment of each edge along the path, with the concentration sampled at the time when the evacuee enters that segment multiplied by the time spent on that segment.

Figure 4 illustrates the grid-cell segmentation.

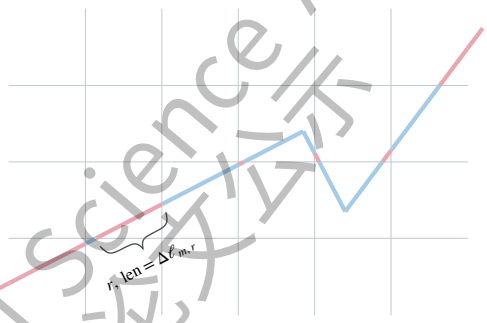


Fig. 4: Grid-cell segmentation of a road polyline. Colors alternate at grid crossings. The brace identifies a segment r of edge e_m, with length $\Delta \ell_{m,r}$.

Therefore, a path passing through downwind high-concentration regions will receive a larger exposure value, even if its geometric distance is short.

Figure 5 separates the cumulative FED score for the standard Yingcai College–Fountain Square route into CO, HCN, and HCl contributions. Departure is at 60 s and travel takes 73.5 s. The full travel interval is shown, including the initial accumulation and subsequent plateau. The contributions sum to approximately 0.6069 at arrival.

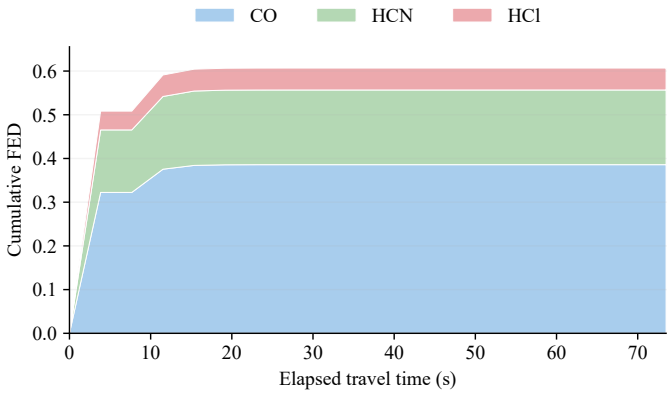


Fig. 5: Stacked cumulative FED contributions over the full Yingcai College–Fountain Square journey. CO is blue, HCN green, and HCl red. The upper boundary gives the total FED score.

2026 S. T. Yau High School Science Award 仅用于2026丘成桐中学科学奖论文公示

D. Narrowest-Road Width Index

The narrowest-road width index is used to describe whether a candidate path contains a road segment with limited walkable space. In this study, each road edge e_m is assigned an effective width W_m with unit m. For a candidate path $p_{h,k}$, the bottleneck width along the path is defined as:

$$W_{\min}(p_{h,k}) = \min_{e_m \in p_{h,k}} W_m \tag{29}$$

Because a smaller bottleneck width should produce a larger negativity in a minimization model, the width term is written as a reciprocal normalized penalty:

$$\frac{W_0}{W_{\min}(p_{h,k})} \tag{30}$$

Here W_0 is the maximum bottleneck width among all feasible candidate paths:

$$W_0 = \max_{k,h} W_{\min}(p_{h,k}) \tag{31}$$

In this way, a path containing a narrower road segment obtains a larger value of the narrowest-road width index.

Figure 6 illustrates this calculation for the standard B4 route from Teaching Building 2 (South exit) to Entrance Road, $66 \to 48 \to 45 \to 44 \to 16 \to 15 \to 14 \to 54 \to 55$. The successive GIS edge widths are $5, 4, 4, 4, 5, 5, 10, 10\,\text{m}$, giving $W_{\min} = 4\,\text{m}$ along the $490.5\,\text{m}$ route. Pink segments identify all three edges attaining the minimum.

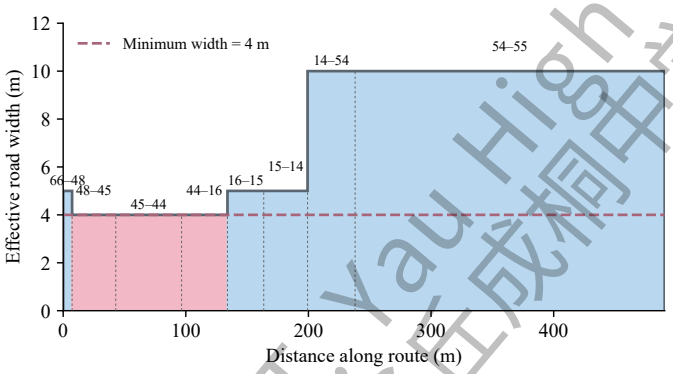


Fig. 6: Effective width along the B4 route from Teaching Building 2 (South exit) to Entrance Road. Edge labels indicate node pairs. Pink segments attain the minimum width of 4 m.

E. Comprehensive Cost Function

The three route indicators $L(p_{h,k})$, $E(p_{h,k})$, and $W_{\min}(p_{h,k})$ have different units and scales. The route length and exposure are normalized by L_0 and E_0, while the bottleneck width is converted into the dimensionless penalty $W_0/W_{\min}(p_{h,k})$. The comprehensive cost of candidate path $p_{h,k}$ is defined as:

$$\text{Cost}(p_{h,k}) = \alpha \frac{L(p_{h,k})}{L_0} + \beta \frac{E(p_{h,k})}{E_0} + \gamma \frac{W_0}{W_{\min}(p_{h,k})} \tag{32}$$

The coefficients α, β, and γ represent the relative importance of distance, toxic exposure, and narrow-road bottlenecks. They are non-negative weights and can be chosen according to evacuation priority. For example, if avoiding toxic gas is the main concern, β should be assigned a larger value.

For the case calculation, the coefficients and normalization parameters are set as shown in Table III. The weights satisfy $\alpha + \beta + \gamma = 1$, with exposure receiving the largest weight.

TABLE III: Case settings of coefficients and normalization parameters in Model 3

Parameter	Value	Meaning
α	0.15	Route length weight
β	0.70	FED exposure weight
γ	0.15	Width penalty weight
L_0	$\max_{k,h} L(p_{h,k})$	Reference path length among all feasible candidate paths.
E_0	$\max_{k,h} E(p_{h,k})$	Reference exposure value among all feasible candidate paths.
W_0	$\max_{k,h} W_{\min}(p_{h,k})$	Reference bottleneck width among all feasible candidate paths

If the maximum exposure value is zero in a no-smoke test case, E_0 should be replaced by a small positive reference value to avoid division by zero.

From the graph point of view, this dimensionless cost can also be interpreted as a dynamic path cost because the exposure term changes with the gas concentration field and the departure time. Thus, the static geographical graph is combined with a time-dependent risk layer from Model 2, and different evacuation plans can be compared under the same cost scale.

F. Route Optimization

For each people cluster k, the best evacuation path is the candidate path with the minimum comprehensive cost:

$$p_k^* = \arg \min_{p_{h,k} \in \mathcal{P}_k} \text{Cost}(p_{h,k}) \tag{33}$$

In this study, risk-weighted Dijkstra generates feasible routes on the road graph; each route is then evaluated by the cost function above, and the minimum-cost feasible route is retained. The total search space of the optimization problem is usually less than 10^5 for a common campus. The method is applied to each building cluster and assembly point before capacity reassignment.

G. Multiple Route Optimization

The multiple-route optimization procedure extends the single-route optimization process to all population clusters k. First, an optimal evacuation route is computed for each cluster based on the integrated cost function. Then, the capacity constraint of each assembly point is checked. If an assembly point becomes overloaded, the farthest route assigned to this point is reassigned to its next-best feasible safe point. This process is repeated until all assembly points satisfy their capacity limits or no feasible alternative route remains.

2026 S.-T. Yau High School Science Award
仅用于2026丘成桐中学科学奖论文评审

VIII. Simulation Process

A. Preparation of the Local GIS Dataset

The case study is based on the real campus spatial data of Beijing 101 High School. Geographic features were first collected from OpenStreetMap (OSM), then checked and edited in QGIS, and entered into the simulation program with gas parameters in a self-developed python-based framework [8].

The final GIS input used in this section consists of two CSV files, `nodes_raw_snapped.csv` and `edges_raw_snapped.csv`. The node table stores the projected planar coordinates (x_k, y_k), node label, node type, and population or capacity attribute P_k. The edge table stores the start node, end node, road length, effective road width W_m, and the geometry of each polyline segment. Because the coordinates are already expressed in meters, the road-network distance, diffusion-grid size, and evacuation path length can be calculated without an additional geographic projection step.

The principal counts and measurement ranges of the processed dataset are summarized in Table IV.

TABLE IV: Summary of the processed Beijing 101 High School GIS dataset

Item	Value
Metadata	
Data Source	OpenStreetMap
MainGeodetic Coordinate System	EPSG:32650
– *Unit*	Meter
Map Size	
Map size	371.374m × 801.734m
Coordinate range of x	439901.434–440272.808 m
Coordinate range of y	4427585.991–4428387.725 m
Nodes Data	
Total number	68
– *Number of buildings*	10
– *Number of midpoints*	47
– *Number of assembly points*	11
Edges Data	
Number of edges	85
Total road length	3600.56 m
Mean edge length	42.36 m
Road width range	2.5–10.0 m
Mean edge width	5.83 m
Populations	
Total positive demand	5090 persons
– *Students*	4790 persons
– *Teachers*	300 persons
Finite assembly capacity	12300 persons

B. The Map of Beijing 101 High School

Figure 7 combines the 68 nodes and 85 edges of the standard-model CSV network in one map. Node labels give node IDs, with English place names and the original population or capacity entries P retained where available. Edge labels give the CSV feature ID and segment index and are placed at edge midpoints. Road-node labels are centered on their nodes. Larger building and assembly-point labels are displaced where needed and linked to their nodes by leader lines. Coordinates are expressed in meters relative to the minimum easting and northing of the input nodes.

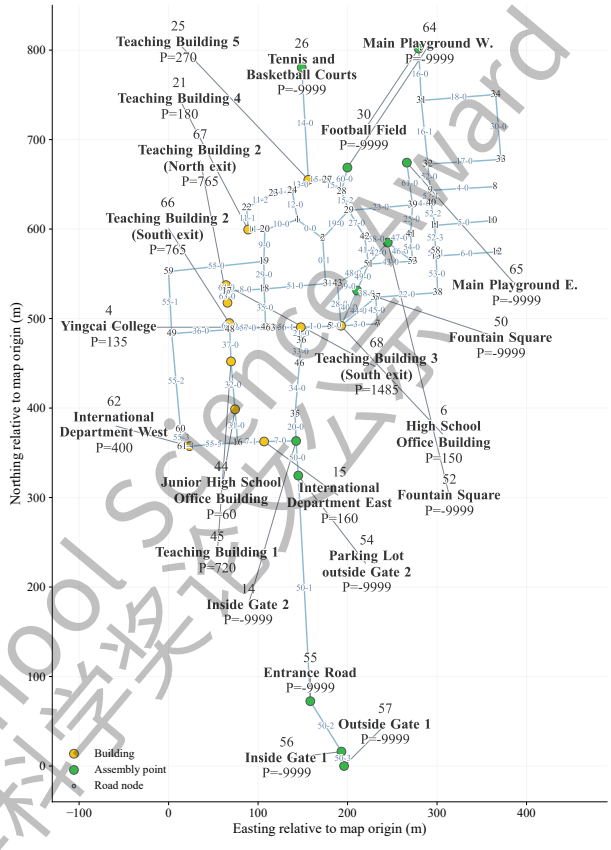


Fig. 7: Combined node and edge representation of the Beijing 101 High School campus road network.

C. Node Classification and Evacuation Demand

Each node in the GIS graph is classified as a building node, a road midpoint, or an assembly point. Building nodes are the starting points of evacuation clusters, typically are main exit or multiple main exits. Their P_k values are positive and represent the estimated number of people who need to leave from the corresponding building entrance. Assembly nodes are the endpoints of evacuation. Their P_k values are negative in the CSV file, and the absolute value is used as the remaining receiving capacity. One assembly node outside the first gate is assigned a very large negative value, so it is interpreted as an external safe outlet with practically unlimited capacity in the route-allocation process.

The 11 building nodes used as possible fire-source locations and evacuation origins are shown in Table V.

D. Road Width and Bottleneck Preparation

The width field in `edges_raw_snapped.csv` is used directly as the effective walkable width W_m. Therefore, the congestion-related term in Model 3 is determined from the narrowest edge on a candidate path:

2026 S-T. Yau High School Science Award
仅用于2026丘成桐中学科学奖公示

TABLE V: Building nodes and evacuation demand in the local GIS dataset

ID	Building node	P_k
4	英才学院 (Yingcai College)	135
6	高中办公楼 (Main High School Office Building)	150
15	国际部东区 (International Department East Area)	160
21	第四教学楼 (NO.4 Teaching Building)	180
25	第五教学楼 (NO.5 Teaching Building)	270
44	初中办公楼 (Office Building for Junior High School)	60
45	第一教学楼 (NO.1 Teaching Building)	720
62	国际部西区 (International Department West Area)	400
66	第二教学楼 S (NO.2 Teaching Building S.)	765
67	第二教学楼 N (NO.2 Teaching Building N.)	765
68	第三教学楼 S (NO.3 Teaching Building S.)	1485

$$W_{\min}(p_{h,k}) = \min_{e_m \in p_{h,k}} W_m \tag{34}$$

The processed GIS data contain no missing road-width records. Most campus paths are 5 m wide, while several main corridors and open routes are wider. Narrow paths with widths of 2.5-4 m are kept in the graph because they may become important bottlenecks in evacuation.

The distribution of the effective road-width values is reported in Table VI.

TABLE VI: Distribution of effective road widths in the processed edge table

W_m (m)	2.5	3.0	4.0	5.0	7.0	9.0	10.0
Number of edges	3	5	4	44	16	5	8

E. Case Definition Before Simulation

The case pipeline selects a source cell, generates gas source terms, advances the diffusion field, then evaluates feasible routes by length, FED exposure, road width, and assembly capacity. The implementation uses risk-weighted Dijkstra for the all-building case and reroutes assignments when a destination is overloaded. Outputs are the destination, length, travel time, exposure, bottleneck width, and comprehensive cost.

F. Parameter Configuration

For the exported simulation case, $\Delta x = \Delta y = 5.0\,\mathrm{m}$, the simulated time interval is $[0, 600]\,\mathrm{s}$, and $\Delta t = 0.1\,\mathrm{s}$. Route exposure is evaluated from $t_{\mathrm{evac}} = 60.0\,\mathrm{s}$. The road graph and gas-specific parameters used by the case are summarized below.

TABLE VII: Hazardous-gas parameters used in the Yingcai College case

Parameter	CO	HCN	HCl
q_g ($\mathrm{kg\,s^{-1}\,kg^{-1}}$)	0.0020	0.0005	0.0080
M_g (kg)	3000	500	700
A_s ($\mathrm{m^2}$)	25	25	25
$D_{\mathrm{eff},g}$ ($\mathrm{m^2/s}$)	0.0012	0.0001	0.0009
λ_g ($\mathrm{s^{-1}}$)	0.0010	0.0015	0.0200
$\widehat{H}_g$ (ppm min)	28300	2730	114000

The table reports the literature-scale $\widehat{H}_g$; the converted H_g is used in the FED calculation. The case weights are $\alpha = 0.15$, $\beta = 0.70$, and $\gamma = 0.15$, so the results are comparative risk rankings.

IX. Case Simulation: Yingcai College Fire under Wind Point to South

This case studies a fire accident in Yingcai College, under typically uniform wind point to the south.

A. Case Setting

Assume that Yingcai College becomes the fire source. The corresponding source cell is selected from the processed campus grid, and the gas inputs are those listed in Table VII.

The wind field is set as a uniform background wind in this baseline simulation. The horizontal wind vector is:

$$\vec{w} = \langle u, v \rangle = \langle 0.1, 0.5 \rangle\ \mathrm{m/s} \tag{35}$$

where the positive u-direction follows the local x-axis of the GIS map and the positive v-direction follows the local y-axis. In other words, this wind is mostly point to south and a little bit east. This wind field transports the plume downwind while diffusion spreads it to neighboring grid cells. Therefore, the hazardous-gas release and the wind field together determine the shape of the plume, and the resulting time-dependent concentration fields are later sampled by Model 3 when evacuation paths are evaluated.

The route-exposure evaluation begins at $t_{\mathrm{evac}} = 60\,\mathrm{s}$, while the gas field is initialized at $t = 0\,\mathrm{s}$ and stored throughout the 600-second simulation.

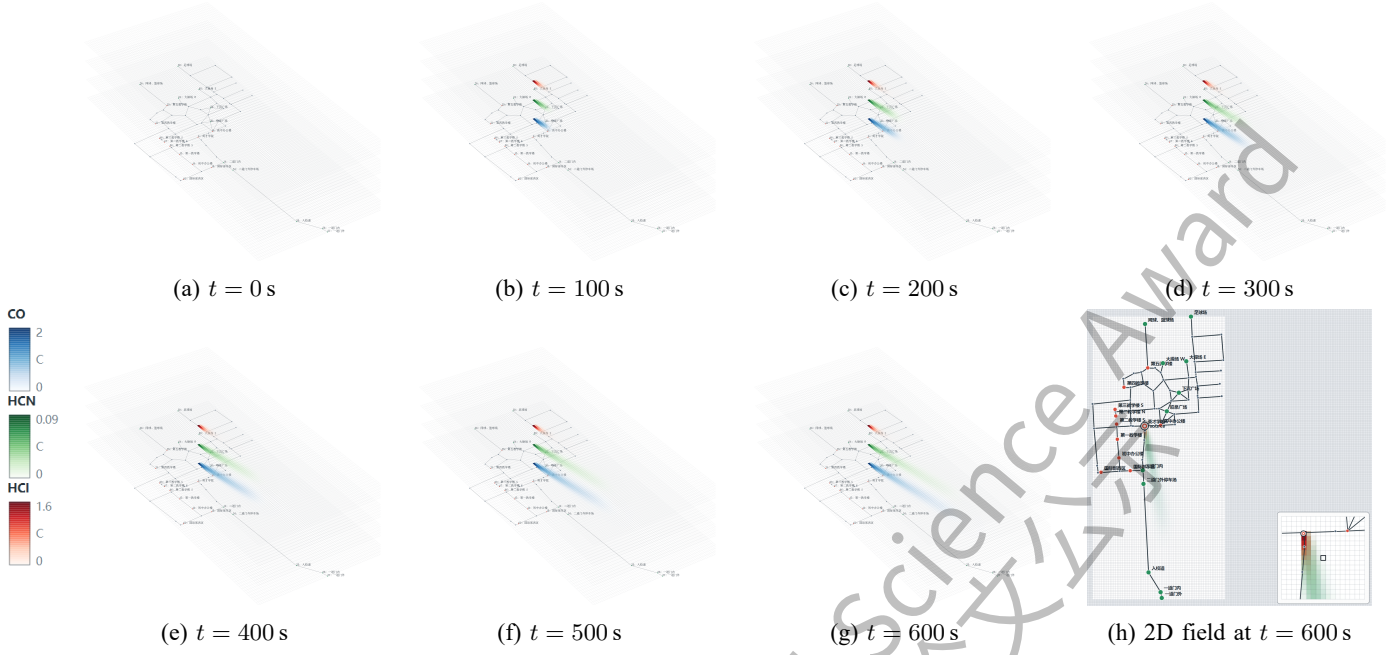
B. Hazardous Gas Diffusion over Time

As shown in Figure 8, the gas concentration is initially concentrated near the source cell and then spreads along the wind direction while gradually diffusing to surrounding cells. Regions closer to the source experience stronger exposure first, while downwind areas become affected later. This diffusion pattern explains why the evacuation risk is spatially nonuniform and why some routes become more dangerous than others as time increases.

C. Evacuation Route Optimization Results

Table VIII and Figure 9 show that the optimized evacuation scheme is not a simple nearest-assembly-point assignment. The capacity constraint redistributes several building clusters from overloaded or less suitable assembly points to alternative safe points, so the final plan uses Fountain Square, the parking lot outside the second gate, the west side of the main playground, and the entrance road at the same time. The reported results include route length, travel time, FED-based exposure, bottleneck width, and the comprehensive cost for each cluster. The rerouted clusters generally accept a longer path in order to satisfy assembly capacity and avoid the higher-risk source region.

2026 S.T. Yau High School Science Award
仅用于2026丘成桐中学科学奖公示



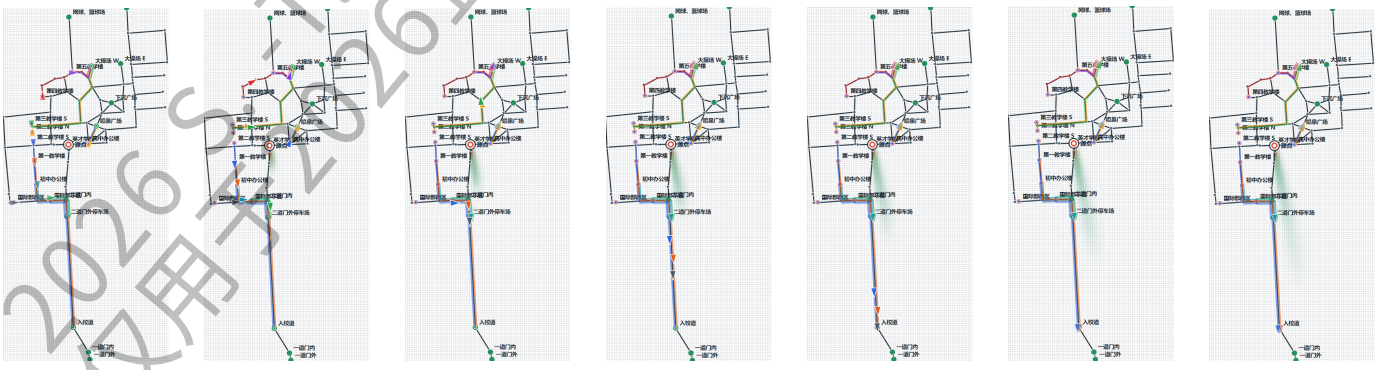
(a) $t = 0\,\mathrm{s}$ (b) $t = 100\,\mathrm{s}$ (c) $t = 200\,\mathrm{s}$ (d) $t = 300\,\mathrm{s}$

(e) $t = 400\,\mathrm{s}$ (f) $t = 500\,\mathrm{s}$ (g) $t = 600\,\mathrm{s}$ (h) 2D field at $t = 600\,\mathrm{s}$

Fig. 8: Evolution of outdoor hazardous-gas concentration distribution. The heat maps show the field from $t = 0$ to $600\,\mathrm{s}$, and the final panel gives the two-dimensional concentration field at $t = 600\,\mathrm{s}$.

TABLE VIII: Evacuation Paths and Cost Parameters Before and After Capacity Rerouting

Building k	Route	Assembly point	P_k	Load/Capacity	$L(p_k)$	$T(p_k)$	$E(p_k)$	$W_{\min}(p_k)$	Cost(p_k, k)	State
Yingcai College	Final	Fountain Square	135	285/500	88.2	73.5	0.607	5	0.3416	ok
High School Office Building	Final	Fountain Square	150	285/500	43.2	36.0	9.714×10^{-11}	5	0.3093	ok
International Department East	Original	Inside Gate 2	160	2105/100	35.7	29.8	2.107×10^{-9}	5	0.3077	overloaded
	Reroute 1	Parking Lot outside Gate 2	160	220/300	74.5	62.1	7.021×10^{-9}	5	0.3160	ok
Teaching Building 4	Final	West Side of Main Playground	180	2700/3000	170.6	142.2	0	5	0.3366	ok
Teaching Building 5	Final	West Side of Main Playground	270	2700/3000	69.3	57.7	0	5	0.3149	ok
Junior High School Office Building	Original	Inside Gate 2	60	2105/100	102.7	85.6	2.867×10^{-6}	4	0.3971	overloaded
	Reroute 1	Parking Lot outside Gate 2	60	220/300	141.5	117.9	9.422×10^{-6}	4	0.4054	ok
Teaching Building 1	Original	Inside Gate 2	720	2105/100	156.4	130.4	3.486×10^{-5}	4	0.4086	overloaded
	Reroute 1	Entrance Road	720	1885/3000	447.7	373.1	0.002209	4	0.4712	ok
International Department West	Original	Inside Gate 2	400	2105/100	119.3	99.4	7.666×10^{-6}	5	0.3256	overloaded
	Reroute 1	Entrance Road	400	1885/3000	410.5	342.1	3.925×10^{-4}	5	0.3882	ok
Teaching Building 2 (South exit)	Original	Inside Gate 2	765	2105/100	199.3	166.1	9.019×10^{-5}	4	0.4178	overloaded
	Reroute 1	Entrance Road	765	1885/3000	490.5	408.8	0.007877	4	0.4806	ok
Teaching Building 2 (North exit)	Original	Fountain Square	765	2535/500	160.3	133.6	4.965×10^{-31}	5	0.3344	overloaded
	Reroute 1	West Side of Main Playground	765	2700/3000	267.3	222.7	4.959×10^{-31}	5	0.3574	ok
Teaching Building 3 (South exit)	Original	Fountain Square	1485	2535/500	154.2	128.5	4.910×10^{-31}	5	0.3331	overloaded
	Reroute 1	West Side of Main Playground	1485	2700/3000	261.2	217.7	4.904×10^{-31}	5	0.3561	ok



(a) $t = 0\,\mathrm{s}$ (b) $t = 100\,\mathrm{s}$ (c) $t = 200\,\mathrm{s}$ (d) $t = 300\,\mathrm{s}$ (e) $t = 400\,\mathrm{s}$ (f) $t = 500\,\mathrm{s}$ (g) $t = 600\,\mathrm{s}$

Fig. 9: Evacuation routes at seven simulation times.

2026 S.T. Yau High School Science Award 仅用于2026丘成桐科学奖论文公示

D. Baseline and Component Comparison

1) Baseline Setting: All variants share the Yingcai College fire source, wind, concentration field, departure time, road network, and demand of 5090 persons. B0 forces every origin to Main Playground by disabling other destinations and selects shortest routes, assuming sufficient playground capacity. B1 minimizes distance, B2 combines distance and exposure, B3 adds width, and B4 additionally enforces assembly capacity. Table IX gives the weights. B2 preserves the length-to-exposure ratio of B3.

TABLE IX: Planning configurations

Variant	α	β	γ	Capacity
B0	1	0	0	Assumed sufficient
B1	1	0	0	Not enforced
B2	$3/17$	$14/17$	0	Not enforced
B3	0.15	0.70	0.15	Not enforced
B4	0.15	0.70	0.15	Enforced

2) Comparison Results: Figure 10 compares time, FED, length, and assembly-point excess load. Each box uses 11 equally weighted final routes. Boxes show quartiles and medians, with whiskers within 1.5 interquartile ranges. Each scatter group contains all 11 assembly points, including unused points. Excess load is the positive difference between assigned demand and capacity, with B0 assigned zero by convention. Travel time is L/s and excludes crowd queues.

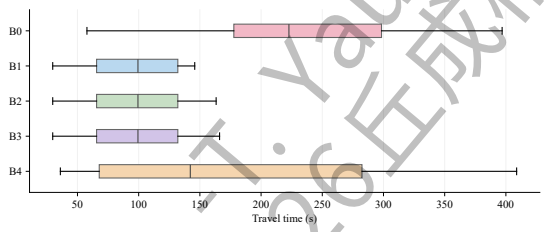
Table X summarizes the outcomes. B1 reduces distance and exposure relative to the fixed-destination B0. B2–B4 share the maximum FED of 0.607, so this metric alone does not resolve their exposure distributions. B2–B3 compare width inclusion at a fixed length-to-exposure ratio, conditional on consistent candidate paths and normalization. B3–B4 compare capacity reassignment at fixed weights. B4 removes 4040 persons of excess load while increasing route length and maximum travel time. These results describe the case-specific trade-off without establishing global optimality of the reassignment heuristic. Detailed assignments appear in Table XI.

TABLE X: Aggregate route-planning outcomes

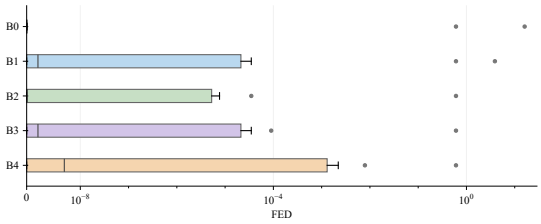
Variant	Length (m)	Max FED	Max time (s)	Excess
B0	3089.3	16.05	396.9	0
B1	1275.0	3.883	145.8	4040
B2	1296.0	0.607	163.3	4040
B3	1299.4	0.607	166.1	4040
B4	2464.5	0.607	408.8	0

TABLE XI: Assembly-point assignments under the five route-planning variants

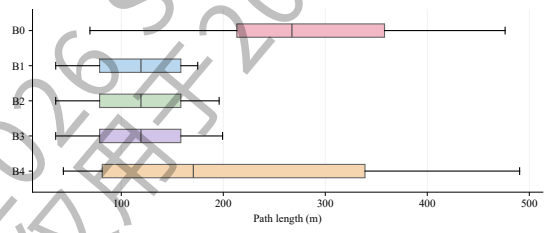
Evacuation origin	**B0**	**B1**	**B2**	**B3**	**B4**
Yingcai College	Playground	Fountain Square	Fountain Square	Fountain Square	Fountain Square
High School Office Building	Playground	Fountain Square	Fountain Square	Fountain Square	Fountain Square
International Department East	Playground	Inside Gate 2	Inside Gate 2	Inside Gate 2	Parking Lot
Teaching Building 4	Playground	Playground W.	Playground W.	Playground W.	Playground W.
Junior's Office Building	Playground	Inside Gate 2	Inside Gate 2	Inside Gate 2	Parking Lot
Teaching Building 1	Playground	Inside Gate 2	Inside Gate 2	Inside Gate 2	Entrance Road
International Department West	Playground	Inside Gate 2	Inside Gate 2	Inside Gate 2	Entrance Road
Teaching Building 2 S.	Playground	Fountain Square	Fountain Square	Inside Gate 2	Entrance Road
Teaching Building 2 N.	Playground	Fountain Square	Fountain Square	Fountain Square	Playground W.
Teaching Building 3 S.	Playground	Fountain Square	Fountain Square	Fountain Square	Playground W.



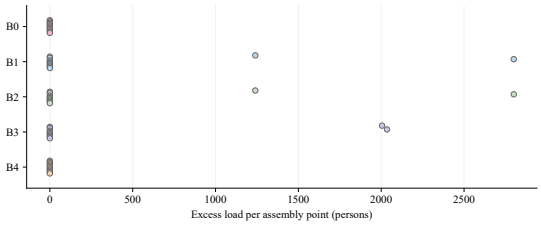
(a) Route travel time.



(b) FED exposure.



(c) Path length.



(d) Excess load per assembly point.

Fig. 10: Baseline and component comparison. FED uses a symmetric logarithmic axis linear below 10^{-8}. Small vertical offsets separate coincident excess-load points. B0 assumes sufficient playground capacity.

2026 S.T. Yau High School Science Award
仅用于2026丘成桐中学科学奖论文公示

X. Discussions

A. Comparison to Peer's Work

Wang et al. couple CFD-predicted time-dependent toxic-gas concentrations with a modified Dijkstra algorithm to minimize inhaled dose during evacuation [9]. The present framework shares this dispersion-to-routing structure, but evaluates campus routes using a weighted combination of length, FED-based exposure, and bottleneck width, followed by assembly-capacity reassignment. This provides an explicit trade-off between exposure and route characteristics; however, the two-dimensional transport model does not resolve the three-dimensional flow effects represented by CFD.

Seo et al. use a CFD-trained neural-network surrogate to predict dynamic risk and integer programming to select evacuation paths [10]. The present model computes the concentration field directly without training a surrogate and uses heuristic capacity reassignment. Its results therefore support campus-specific scenario comparison, while global optimality and performance relative to these existing methods remain unestablished without a common benchmark.

B. Summary and Further Improvement

The proposed framework connects hazardous-gas generation, wind-driven diffusion, and evacuation routing in one computational chain, but several simplifications remain. The gas-generation model uses representative material masses and typical generation rates rather than room-level fuel loads or time-dependent burning rates. The diffusion model is two-dimensional and assumes a near-ground concentration layer, so vertical smoke rise, buoyancy, building wake effects, local turbulence, and obstacle-induced flow separation are not explicitly resolved.

Future work can improve realism by using more detailed fuel-load surveys, CFD-supported or locally measured wind fields, additional fire-effluent species such as CO_2, NO_x, SO_x, soot particles etc., and a more detailed exposure model that includes gas interaction and visibility reduction. The evacuation model can also be extended from building-level clusters to agent-based crowd simulation, including heterogeneous walking speeds, congestion, queues at narrow paths, and dynamic route updates when evacuees observe smoke or blocked roads.

XI. Conclusions

This study develops a GIS-based framework for outdoor campus fire evacuation planning by combining hazardous-gas generation, wind-driven diffusion, and route optimization.

Using Beijing 101 High School as the case study, the method converts campus road data and fire-gas source terms into a time-dependent risk field, then evaluates evacuation paths by route length, toxic exposure, bottleneck road width, and assembly-point capacity.

The case study simulation demonstrates that the more optimized and safer routes can differ from those sharing similar assembly points and may not correspond to the geometrically shortest paths. Plume dispersion, departure timings, road bottlenecks and assembly point capacity all influence evacuation related risk.

The main contribution is a reproducible workflow came from a real problem that turns campus GIS data and fire-gas simulation into quantitative route recommendations, providing a basis for comparing emergency plans and identifying high-risk roads or overloaded safe points.

2026 S. T. Yau High School Science Award
仅用于2026丘成桐中学科学奖论文公示

References

[1] J. M. Stockie, "The mathematics of atmospheric dispersion modeling," *SIAM Review*, vol. 53, no. 2, pp. 349–372, 2011. DOI: 10.1137/10080991X.

[2] P. E. Hart, N. J. Nilsson, and B. Raphael, "A formal basis for the heuristic determination of minimum cost paths," *IEEE Transactions on Systems Science and Cybernetics*, vol. 4, no. 2, pp. 100–107, 1968. DOI: 10.1109/TSSC.1968.300136.

[3] D. A. Purser and J. L. McAllister, "Assessment of hazards to occupants from smoke, toxic gases, and heat," in *SFPE Handbook of Fire Protection Engineering*, 5th, New York, NY, USA: Springer, 2016, ch. 63, pp. 2308–2428. DOI: 10.1007/978-1-4939-2565-0_63. [Online]. Available: https://doi.org/10.1007/978-1-4939-2565-0_63.

[4] S. T. McKenna and T. R. Hull, "The fire toxicity of polyurethane foams," *Fire Science Reviews*, vol. 5, no. 1, p. 3, 2016. DOI: 10.1186/s40038-016-0012-3. [Online]. Available: https://link.springer.com/article/10.1186/s40038-016-0012-3.

[5] R. G. Gann, J. D. Averill, E. L. Johnsson, M. R. Nyden, and R. D. Peacock, "Fire effluent component yields from room-scale fire tests," *Fire and Materials*, vol. 34, no. 6, pp. 285–314, 2010. DOI: 10.1002/fam.1024.

[6] J. E. Doe, "The combustion toxicology of polyvinylchloride revisited," *Journal of Fire Sciences*, vol. 5, no. 4, pp. 268–290, 1987. DOI: 10.1177/073490418700500402. [Online]. Available: https://journals.sagepub.com/doi/10.1177/073490418700500402.

[7] K. McGrattan, S. Hostikka, R. McDermott, J. Floyd, C. Weinschenk, and K. Overholt, "Fire dynamics simulator user's guide," National Institute of Standards and Technology, Tech. Rep. NIST Special Publication 1019, 2017. DOI: 10.6028/NIST.SP.1019. [Online]. Available: https://doi.org/10.6028/NIST.SP.1019.

[8] Y. Chen, *Campus-gas-diffusion-studio.simulation-program-qt*, version 1dcdaa654d38673dbaf67ff17e6a0d8e8264d15d, 2026. [Online]. Available: https://github.com/cyx728/Campus-Gas-Diffusion-Studio.Simulation-Program-qt.

[9] J. Wang, X. Yu, R. Zong, and S. Lu, "Evacuation route optimization under real-time toxic gas dispersion through CFD simulation and Dijkstra algorithm," *Journal of Loss Prevention in the Process Industries*, vol. 76, p. 104 733, 2022. DOI: 10.1016/j.jlp.2022.104733.

[10] S.-K. Seo, Y.-G. Yoon, J.-s. Lee, J. Na, and C.-J. Lee, "Deep neural network-based optimization framework for safety evacuation route during toxic gas leak incidents," *Reliability Engineering & System Safety*, vol. 218, p. 108 102, 2022. DOI: 10.1016/j.ress.2021.108102.

2026 S.-T. Yau High School Science Award
仅用于2026丘成桐中学科学奖论文公示